

Reactions of both aluminum hydride cluster anions and boron aluminum hydride cluster anions with oxygen: Anionic products



Xinxing Zhang^a, Haopeng Wang^a, Gerd Ganteför^b, Bryan W. Eichhorn^c, Kit Bowen^{a,*}

^a Department of Chemistry, Johns Hopkins University, Baltimore, MD 21218, United States

^b Fakultät für Physik, Universität Konstanz, 78457 Konstanz, Germany

^c Department of Chemistry, University of Maryland at College Park, College Park, MD 20742, United States

ARTICLE INFO

Article history:

Received 5 February 2016

Received in revised form 1 April 2016

Accepted 2 April 2016

Available online 7 April 2016

Keywords:

Mass spectrometry

Anions

Clusters

ABSTRACT

The anionic products of reactions between aluminum hydride cluster anions and oxygen and between boron aluminum hydride cluster anions and oxygen were identified by mass spectrometry. While aluminum oxide anions dominated the products of both reactions, low intensities of hydrogen-containing aluminum oxide product anions were also observed in both cases. Surprisingly, in the reactions between boron aluminum hydride cluster anions and oxygen, there was scant evidence for boron-containing anionic products.

© 2016 Elsevier B.V. All rights reserved.

1. Introduction

Boranes (boron hydrides) were once thought to be promising propellants [1–14]. The reasons derived from their relatively light weight and their high energy release upon oxidation, e.g., $\Delta H^\circ_{298} = -482.9$ kcal/mol for the reaction, $B_2H_6(g) + 3O_2(g) \rightarrow B_2O_3(s) + 3H_2O(g)$ [15]. The extraordinary exothermicities of borane oxidation reactions are ultimately driven by the high heat of formation of B_2O_3 . Despite their promise, however, the energy actually released by the oxidation of boranes fell well short of expectations. Rather than burning completely to B_2O_3 , the reaction pathway got caught in kinetic traps, whereby hydrogen-, boron-, and oxygen-containing molecules were formed; these effectively blocked the reaction from proceeding to full oxidation. Collectively, these spoiler molecules were known as HOB0 compounds.

The “HOB0 problem” emerged during the latter half of the 1950’s, during efforts to develop boranes into high performance jet fuels [1]. Ditter and Shapiro [5] reported that the oxidation of pentaborane produced stable hydrogen-, boron-, and oxygen-containing products, among which $H_2B_2O_3$ showed the highest abundance. An additional product, HOB0 was 54.8% as prevalent as $H_2B_2O_3$, while B_2O_3 was only 11.1% as prevalent. Bauer and Wiberley [6] also studied the oxidation products of pentaborane, these being found to be HBO, HOB0, and $H_2B_2O_3$. Baden et al. [7] reported

that the slow oxidation of pentaborane formed diborane, hydrogen, and a white solid. Whatley and Pease [8] studied the products of diborane oxidation. Roth and Baure [9] found HOB0 to be the main product during the oxidation of diborane. Roth and Bauer [10] proposed that the formation of HOB0 severely inhibits the oxidation of boranes by breaking links in its chain reaction mechanism. In summary, boranes never reached their potential as propellants due to the “HOB0 problem”.

As boron’s sister element, aluminum has been widely utilized in propellants, usually in the form of very small particles [16–20]. The best known aluminum hydride analog to the boranes is alane (AlH_3). Unlike boranes, which tend to be gases, alane is a solid with six crystalline phases. In principle, alane is a promising propellant. The specific impulse of an AP/HTPB propellant mixed with alane was calculated to be 100 N s kg^{-1} higher than the same propellant mixed with the same concentration of aluminum [21]. Furthermore, the flame temperature of alane-containing propellants was 15% lower than that of aluminum-containing propellants, resulting in a lower need for thermal protection of the rocket [22]. The mechanism of alane combustion was proposed to be: $AlH_3 \rightarrow Al + 3/2 H_2$ (dehydrogenation), followed by $Al + 3/4 O_2 \rightarrow 1/2 Al_2O_3$ (oxidation) [23]. Both the hydrogen release temperature and the ignition temperature were lower than aluminum’s melting point [22]. Despite these advantages, however, alane has seen relatively little use as an ingredient in propellants. Its Achilles heel appears to be its poor thermal stability, although materials purity issues may have also contributed to its lack of acceptance as a propellant [22,24].

* Corresponding author.

E-mail address: kbowen@jhu.edu (K. Bowen).

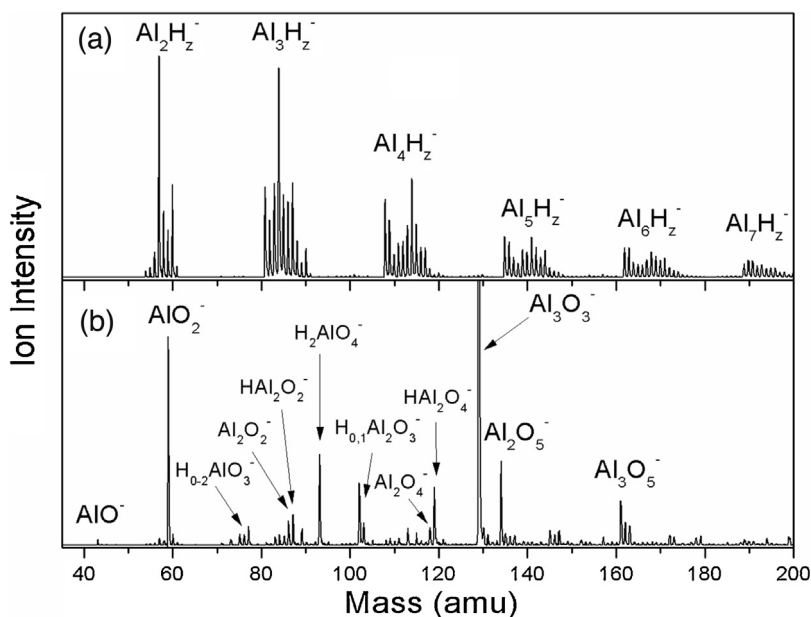


Fig. 1. Typical mass spectra of Al_yH_z^- : (a) before the addition of O_2 into the reaction cell and (b) after the addition of O_2 into the reaction cell, i.e., the anionic reaction products.

While alane is the only aluminum hydride to have been studied in macroscopic quantities, aluminum hydride cluster anions, Al_yH_z^- , have been prepared and extensively characterized in molecular beam environments. Al_4H_6 cluster was reported to have exceptional stability, and its heat of combustion was calculated to be 438 kcal/mol, i.e., ~ 2.6 times greater than that of methane [25]. Subsequent studies discovered and characterized hundreds of previously unknown aluminum hydride cluster anions, Al_yH_z^- [26–32]. Additionally, about 80 boron aluminum hydride cluster anions, $\text{B}_x\text{Al}_y\text{H}_z^-$, have also been discovered and characterized [33].

The availability of aluminum hydride cluster anion beams makes it possible to determine whether the products of reactions between Al_yH_z^- and O_2 exhibit a “HOAIO problem”. Likewise, the availability of boron aluminum hydride cluster anion beams makes it possible to determine whether the products of reactions between $\text{B}_x\text{Al}_y\text{H}_z^-$ and O_2 exhibit a “HOAIO problem”, a “HOBO problem”, or both. Intuition suggests that reactions between Al_yH_z^- and O_2 will go to complete oxidation, avoiding a hypothetical “HOAIO problem”. Given this expectation and the history of HOBO formation in reactions between boranes and O_2 , it is interesting to consider whether the presence of aluminum in $\text{B}_x\text{Al}_y\text{H}_z^-$ might carry its boron moiety along with it to complete oxidation during reactions between $\text{B}_x\text{Al}_y\text{H}_z^-$ and O_2 , or whether the formation of HOBO-like products will continue to prove resilient. Can reactions between $\text{B}_x\text{Al}_y\text{H}_z^-$ and O_2 bypass the “HOBO problem”?

In the present work, we determine the identities of the anionic products of reactions between Al_yH_z^- and O_2 and between $\text{B}_x\text{Al}_y\text{H}_z^-$ and O_2 . This is accomplished by directing cluster anion beams through a low-density reaction cell containing O_2 , after which the emerging anionic products are identified by mass spectrometry. This methodology allows us to detect and identify the anionic forms of any HOAIO and/or HOBO products formed by these reactions. Previous studies of borane oxidation used mass spectrometry to identify the cations of neutral HOBO products. Here, our use of mass spectrometry to identify the anionic products of Al_yH_z^- and $\text{B}_x\text{Al}_y\text{H}_z^-$ oxidation reactions is potentially a more sensitive method of detecting HOAIO and HOBO molecules, given that aluminum and boron compounds tend to be electrophilic and thus to readily form negative ions.

2. Experimental and computational methods

Both aluminum hydride and boron aluminum hydride cluster anions, Al_yH_z^- and $\text{B}_x\text{Al}_y\text{H}_z^-$, were generated in a pulsed arc cluster ionization source (PACIS), which has proven to be a powerful tool for generating metal and metal hydride cluster anions [25,33–44]. Briefly, a ~ 30 μs duration, 150 V electrical pulse applied across the anode and the sample cathode vaporizes the sample atoms and forms a plasma. In the present case, the sample cathode is a 0.5 in. diameter pure aluminum rod or alternatively a boron/aluminum powder mixture which had been firmly pressed onto a shallow cup in the top of the aluminum rod. About 200 psi of ultrahigh purity hydrogen gas was then injected through a pulsed valve into the arc region, where it was dissociated into hydrogen atoms, before the resulting plasma/gas mixture was propelled down a 3 cm diameter tube. Cluster anions generated in this way then drifted through a gap before entering the 10 cm long, 1 cm diameter reaction cell with 2 mm diameter apertures on both ends. Next, ~ 50 psi of oxygen was injected into the cell by another pulsed valve located on the side of the reaction cell. The two end-apertures helped to contain the oxygen and to limit any back flow. With no oxygen in the cell, Al_yH_z^- or $\text{B}_x\text{Al}_y\text{H}_z^-$ species continued on into the extraction grids of a time-of-flight mass spectrometer, where they were identified, but when oxygen was added to the cell and anionic reaction products were formed, they too were identified by mass spectrometry.

In the cases of the anionic HOAIO products, it was also of interest to characterize their geometries. Density functional theory calculations were conducted by applying Becke’s three-parameter hybrid functional (B3LYP)[45–47] using the Gaussian09 software package [48] to determine the geometries of anionic H_2AlO_4^- and HAl_2O_4^- . All geometries were fully optimized using the 6-311++G (3df, 3pd) basis set.

3. Results

Fig. 1(a) shows a typical mass spectrum of Al_yH_z^- ($y=2-7$), produced by the PACIS source. Fig. 1(b) presents the same mass spectral range, once O_2 has been introduced into the reaction cell. While many different anionic products appeared in Fig. 1(b), including AlO^- , AlO_2^- , $\text{H}_{0.2}\text{AlO}_3^-$, $\text{H}_{0.1}\text{Al}_2\text{O}_2^-$, H_2AlO_4^- ,

Table 1

The relative intensities of the major anionic products due to reactions between aluminum cluster anions and oxygen. The intensity of Al_3O_3^- is set to be 100%.

Species	Mass (amu)	Relative intensity (%)
Al_3O_3^-	129	100.0
AlO_2^-	59	43.9
H_2AlO_4^-	93	19.0
Al_2O_5^-	134	17.9
Al_2O_3^-	102	13.1
HAL_2O_4^-	119	12.3
Al_3O_5^-	161	9.2
HAL_2O_2^-	87	6.4
Al_2O_2^-	86	5.0
HAL_2O_3^-	103	4.8
H_2AlO_3^-	77	3.9
Al_2O_4^-	118	3.6
AlO_3^-	75	2.2
HALO_3^-	76	2.0
AlO^-	43	1.1

Table 2

The relative intensities of the major anionic products due to reactions between boron aluminum cluster anions and oxygen. The intensity of Al_3O_3^- is set to be 100%.

Species	Mass (amu)	Relative intensity (%)
Al_3O_3^-	129	100.0
Al_2O_5^-	134	58.2
AlO_2^-	59	56.4
Al_3O_5^-	161	28.4
Al_2O_3^-	102	26.1
HAL_2O_4^-	119	14.4
AlO_3^-	75	13.8
Al_2O_4^-	118	13.7
Al_3O_4^-	145	13.3
H_2AlO_4^-	93	10.2
AlO^-	43	3.2
BO_2^-	42 and 43	2.9

$\text{H}_{0,1}\text{Al}_2\text{O}_3^-$, $\text{H}_{0,1}\text{Al}_2\text{O}_4^-$, Al_3O_3^- , Al_2O_5^- , and Al_3O_5^- , the most intense among them was Al_3O_3^- . Setting the intensity of Al_3O_3^- at 100%, the relative intensities of the other anionic products are listed in Table 1. The most abundant HOAlO-type products are H_2AlO_4^- and HAL_2O_4^- , these being 19% and 12% of the intensity of Al_3O_3^- , respectively. Additional HOAlO-type anionic products were HAL_2O_2^- , HAL_2O_3^- , H_2AlO_3^- , and HALO_3^- , although their intensities are weaker. Both of these “before” and “after” mass spectra have been repeated many times in close sequence. Furthermore, the product anion relative intensities reported in Table 1 were relatively constant from run to run. The unmarked mass peaks in Fig. 1(b) are likely due to unreacted aluminum hydride cluster anions, all of which exhibit very low intensities. It is clear, however, that most aluminum hydride cluster anions had burned.

Fig. 2(a) shows a typical mass spectrum of $\text{B}_x\text{Al}_y\text{H}_z^-$ ($x=2, 3$), these species having also been generated in the PACIS source. While Al_yH_z^- species are present there, the $\text{B}_x\text{Al}_y\text{H}_z^-$ ($x=2, 3$) species clearly dominate. Fig. 2(b) presents the same mass spectrum, once O_2 has been introduced into the reaction cell. The anions appearing in Fig. 2(b) included BO_2^- , AlO^- , AlO_2^- , AlO_3^- , H_2AlO_4^- , Al_2O_3^- , $\text{H}_{0,1}\text{Al}_2\text{O}_4^-$, Al_3O_3^- , Al_2O_5^- , Al_3O_4^- , and Al_3O_5^- , with Al_3O_3^- again exhibiting the highest intensity. Many of the species seen in Fig. 1(b) are also present in Fig. 2(b). Setting the intensity of Al_3O_3^- at 100%, the relative intensities of the other anionic products in Fig. 2(b) are listed in Table 2. Like the mass spectra of Fig. 1(a) and (b), the mass spectra of Fig. 2(a) and (b) have been repeated many times in close sequence. Again, the product anion relative intensities reported in Table 2 were relatively constant from run to run. Unmarked mass peaks in Fig. 2(b) may well be unreacted cluster anions of the types seen in Fig. 2(a).

Mass coincidences significantly complicate the delineation between boron-containing and aluminum-containing species, e.g.,

the masses of ^{11}BO and of Al are the same. Nevertheless, the presence of ^{10}B , which is 24.7% as abundant as ^{11}B , helps to sort out some mass coincidences. For example, while the masses of AlO^- and $^{11}\text{BO}_2^-$ are the same (43 amu), the appearance in Fig. 2(b) of a mass peak at 42 amu, i.e., $^{10}\text{BO}_2^-$, strongly suggests that BO_2^- is present [see inset in Fig. 2(b)]. On the other hand, the mass of AlO_2^- is the same as that of $^{11}\text{BO}_3^-$ (59 amu), but since there is no significant intensity at 58 amu, it is clear that BO_3^- is not present in the mass spectrum.

There are two types of boron-containing species that might reasonably be expected to appear in Fig. 2(b) in addition to aluminum oxide anions, HOAlO-type anions, and unreacted $\text{B}_2\text{Al}_y\text{H}_z^-$, $\text{B}_3\text{Al}_y\text{H}_z^-$, and Al_yH_z^- species. These are boron oxide anions and HOBO-type anions. Numerous prominent aluminum oxide anion peaks do indeed appear in Fig. 2(b). Focusing on the stoichiometries of those aluminum oxide anions as guides, we examined the mass spectrum in Fig. 2(b), looking for the presence of boron oxide anion analogs to Al_3O_3^- , Al_2O_5^- , Al_3O_5^- , Al_2O_3^- , AlO_2^- , Al_2O_4^- , Al_3O_4^- , and AlO_3^- . The most intense mass spectral aluminum oxide anion peak is that of Al_3O_3^- . Its boron counterpart, B_3O_3^- , should appear over the mass range, 78–81 amu. Upon magnifying the mass spectrum in Fig. 2(b), we saw only weak intensity peaks in this mass range, and these also exhibited the wrong isotope pattern. Moreover, upon magnifying Fig. 2(a), we also saw mass peaks of unreacted species at these same masses. Except for BO_2^- , the same conclusions were reached for B_2O_5^- , B_3O_5^- , B_2O_3^- , BO_2^- , B_2O_4^- , B_3O_4^- , and BO_3^- . They were either absent or mistaken for unreacted species: again, see Fig. 2(a). Even if some of them did occur in the mass spectrum, it is clear that their intensities were quite weak.

We also searched the magnified mass spectrum of Fig. 2(b), looking for HOBO-type anions. Again, we took our clue from the stoichiometries of HOAlO-type anions that are present in Fig. 2(b), i.e., H_2AlO_4^- and HAL_2O_4^- . The mass positions of both H_2BO_4^- (76 & 77 amu) and HB_2O_4^- (85–87 amu) show peaks with enticing isotope patterns, but their intensities are weak, and at best they may be entangled with peaks from unreacted species; cf., Fig. 2(a). For both boron oxide anions and HOBO-type anions in Fig. 2(b), most of them were either absent or present only at low intensities, where even those may have been obscured by unreacted anions as seen in Fig. 2(a). Surprisingly, there is little evidence of boron-containing anionic species in Fig. 2(b).

4. Discussion

The majority of the anionic products observed due to the oxidation of aluminum hydride and boron aluminum hydride anions were aluminum oxide (cluster) anions. In some of these, e.g., AlO_2^- and Al_3O_5^- , aluminum is in its highest oxidation state. However, in its most abundant product, Al_3O_3^- , it is not. The Al_3O_3^- ion can be viewed as $(\text{Al}_3)^{5+} (\text{O}^{2-})_3^-$ [49], and its unusual stability can be attributed to its six member ring structure. Also, while Al_2O_3 , with its $\text{Al}(+3)$ oxidation state, would be expected to be the favored (most stable) neutral product in aluminum compound oxidation reactions, the Al_2O_3^- anion, with its additional electron and thus its lower Al oxidation state, is not [50].

While aluminum oxide anions were clearly the dominate reaction products of the oxidation of both aluminum hydride and boron aluminum hydride anions, low intensities of HOAlO product anions were also observed in both cases. The hydrogen-containing, aluminum oxide product anions, H_2AlO_4^- and HAL_2O_4^- are representative. Their calculated structures are presented in Fig. 3, where all bond lengths are given in Angstroms, Å. H_2AlO_4^- has a tetrahedral structure, where two hydroxyl groups and a peroxide moiety are attached to the central aluminum atom. Its vertical detach-

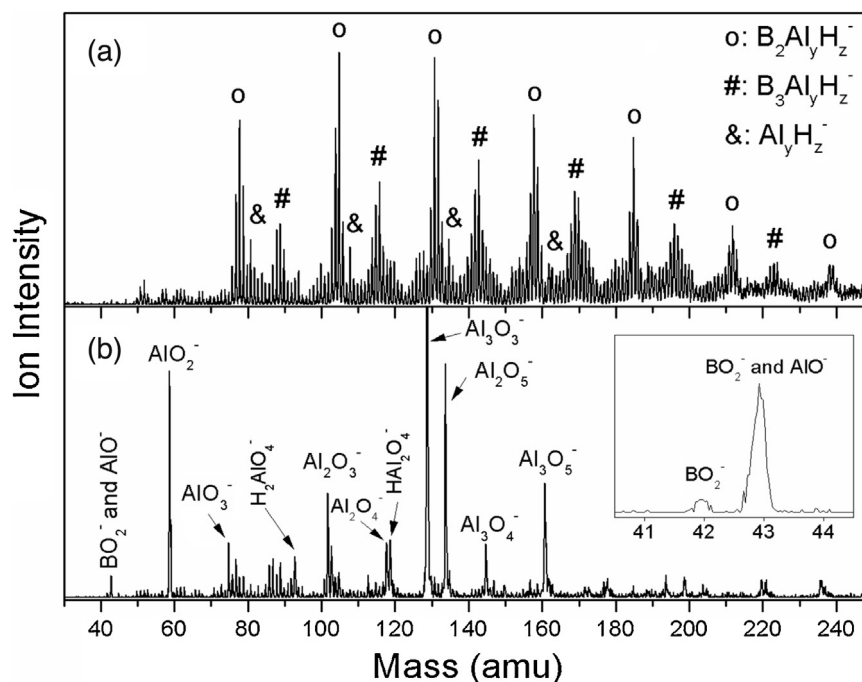


Fig. 2. Typical mass spectra of $B_xAl_zH_y^-$ and $Al_zH_y^-$: (a) before the addition of O_2 into the reaction cell and (b) after the addition of O_2 into the reaction cell, i.e., the anionic reaction products. The embedded mass spectrum in (b) shows the presence of BO_2^- along with AlO^- .

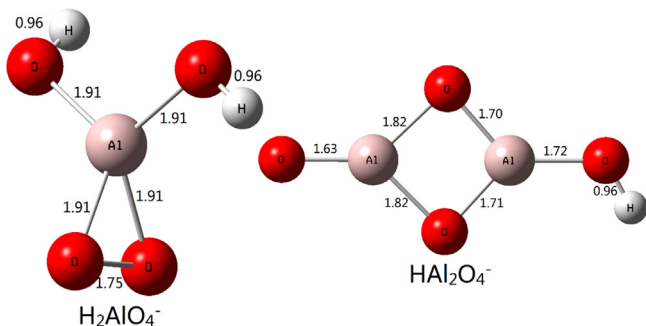


Fig. 3. Calculated structures of $H_2AlO_4^-$ and $HAl_2O_4^-$. All the bond lengths are in Å.

ment energy was calculated to be 3.73 eV. $HAl_2O_4^-$ is planar, with the two aluminum atoms connected through two bridging oxygen atoms and with one oxygen atom and one hydroxyl group forming radial bonds with the two aluminum atoms. Its vertical detachment energy was calculated to be 3.78 eV. Thus, contrary to conventional wisdom, the oxidation of aluminum hydride (cluster) anions does have a “HOB0-like problem”, i.e., the appearance of HOAlO-type anion products, although it is quite minor compared to the dominant HOB0-type products observed due to the oxidation of boranes.

Despite our experiments being repeated many times, we observed little evidence for the presence of boron in the mass spectrum presented in Fig. 2(b). Specifically, other than BO_2^- , we saw no definitive evidence for other boron oxide anions or for HOB0-type anions in Fig. 2(b). Where is the boron? Perhaps, boron-containing anionic species are hidden by mass coincidences or buried under the mass peaks of unreacted species. It seems more likely that the boron-containing molecules are present as neutral products. During long boron aluminum hydride runs, the downstream window became thinly coated with a brown film, suggesting the deposition of neutral products. With the same exposure time, this does not happen during aluminum hydride runs. Still, the “boron dark

matter” dilemma remains unsatisfactorily explained; it will be the subject of future experiments in our lab.

When we began these anion reactivity studies, we hypothesized that the oxidation of aluminum hydride (cluster) anions would not exhibit a HOB0-like problem, i.e., a HOAlO-type problem, focusing our attention on whether the oxidation of boron aluminum hydride anions might bypass the “HOB0 problem”. We learned instead that the oxidation of aluminum hydride (cluster) anions does in fact exhibit a “HOB0-type problem”, although only mildly compared to that seen in the oxidation of boranes. The idea of using boron aluminum hydrides to minimize or even eliminate the “HOB0 problem” also dealt us surprises. While we did not see evidence of HOB0-like anionic species, we also could not account for the disposition of boron generally, e.g., as boron oxide anions.

Acknowledgement

This material is based upon work supported by the Air Force Office of Scientific Research (AFOSR), under Grant Number FA9550-14-1-0324 (K.H.B.).

References

- [1] A. Dequasia, *The Green Flame: Surviving Government Secrecy*, American Chemical Society, Washington, DC, 1991.
- [2] W.N. Lipscomb, *Boron Hydrides*, W. A. Benjamin Inc., New York, 1963.
- [3] N. Greenwood, A. E. Chemistry of the Elements, 2nd ed., Elsevier Science Amsterdam, The Netherlands, 1997.
- [4] A. Stock, C. Massenez, *Ber. Dtsch. Chem. Ges.* 45 (1912) 3539.
- [5] J.F. Ditter, I. Shapiro, *J. Am. Chem. Soc.* 81 (1959) 1022.
- [6] W.H. Bauer, S. Wiberley, *Borax to Boranes*, Advances in Chemistry American Chemical Society, Washington, DC, 1961.
- [7] H.C. Baden, S.E. Wiberley, W.H. Bauer, *J. Phys. Chem.* 59 (1955) 287.
- [8] A.T. Whatley, R.N. Pease, *J. Am. Chem. Soc.* 76 (1954) 1997.
- [9] W. Roth, W.H. Bauer, *J. Phys. Chem.* 60 (1956) 639.
- [10] W. Roth, W.H. Bauer, *Fifth Symposium on Combustion*, Reinhold New York, 1955, p. 710.
- [11] F.P. Price, *J. Am. Chem. Soc.* 72 (1950) 5361.
- [12] H.C. Baden, W.H. Bauer, S.E. Wiberley, *J. Phys. Chem.* 62 (1958) 331.
- [13] F.P. Price, *J. Am. Chem. Soc.* 73 (1951) 2141.
- [14] E. Gobbett, J.W. Linnett, *J. Chem. Soc.* (1962) 2893.

- [15] F.D. Rossini, Selected Values of Chemical Thermodynamic Properties, Natl. Bur. Standards Circular No. 300, 1952.
- [16] A. Rai, D. Lee, K. Park, M.R. Zachariah, *J. Phys. Chem. B* 108 (2004) 14793.
- [17] A. Rai, K. Park, L. Zhou, M.R. Zachariah, *Combust. Theory Model.* 10 (2006) 843.
- [18] G.V. Ivanov, F. Tepper, 4th Int. Symp. Spec. Top. Chem. Propul., 636, 1997.
- [19] C.E. Aumann, G.L. Skofronick, J.A. Martin, *J. Vac. Sci. Technol. B* 13 (1995) 1178.
- [20] T. Bazyn, H. Krier, N. Glumac, *Combust. Flame* 145 (2006) 703.
- [21] V. Weiser, N. Eisenreich, A. Koleczko, E. Roth, *Propellants Explos. Pyrotech.* 32 (2007) 213.
- [22] G. Young, N. Piekielek, S. Chowdhury, M.R. Zachariah, *Combust. Sci. Technol.* 182 (2010) 1341.
- [23] T. Bazyn, R. Eyer, H. Krier, N. Glumac, *J. Propuls. Power* 20 (2004) 427.
- [24] J. Graetz, J.J. Reilly, *J. Phys. Chem. B* 109 (2005) 22181.
- [25] X. Li, A. Grubisic, S.T. Stokes, J. Cordes, G.F. Gantefoer, K.H. Bowen, B. Kiran, M. Willis, P. Jena, R. Burgert, H. Schnoekel, *Science* 315 (2007) 356.
- [26] P.J. Roach, A.C. Reber, W.H. Woodward, S.N. Khanna, A.W. Castleman Jr., *Proc. Natl. Acad. Sci.* 104 (2007) 14565.
- [27] B. Kiran, P. Jena, X. Li, A. Grubisic, S.T. Stokes, G.F. Gantefoer, K.H. Bowen, R. Burgert, H. Schnoekel, *Phys. Rev. Lett.* 98 (2007) 256802.
- [28] A. Grubisic, X. Li, G.F. Gantefoer, K.H. Bowen, B. Kiran, P. Jena, R. Burgert, H. Schnoekel, *J. Am. Chem. Soc.* 129 (2007) 5969.
- [29] A. Grubisic, X. Li, S.T. Stokes, K. Vetter, G.F. Gantefoer, K.H. Bowen, P. Jena, B. Kiran, R. Burgert, H. Schnoekel, *J. Chem. Phys.* 131 (2009) 121103.
- [30] X. Li, A. Grubisic, K.H. Bowen, A.K. Kandalam, B. Kiran, G.F. Gantefoer, P. Jena, *J. Chem. Phys.* 132 (2010) 241103.
- [31] X. Zhang, H. Wang, E. Collins, A. Lim, G. Ganteför, B. Kiran, H. Schnöckel, B. Eichhorn, K.H. Bowen, *J. Chem. Phys.* 138 (2013) 124303.
- [32] J.D. Graham, A.M. Buytendyk, X. Zhang, E.L. Collins, K. Boggavarapu, G. Gantefoer, B.W. Eichhorn, G.L. Gutsev, S. Behera, P. Jena, K.H. Bowen, *J. Phys. Chem. A* 118 (2014) 8158.
- [33] H. Wang, X. Zhang, Y. Ko, G.F. Ganteför, K.H. Bowen, X. Li, K. Boggavarapu, A. Kandalam, *J. Chem. Phys.* 140 (2014) 164317.
- [34] X. Zhang, Y. Wang, H. Wang, A. Lim, G. Ganteför, K.H. Bowen, J.U. Reveles, S.N. Khanna, *J. Am. Chem. Soc.* 135 (2013) 4856.
- [35] X. Zhang, P. Robinson, G. Gantefoer, A. Alexandrova, K.H. Bowen, *J. Chem. Phys.* 143 (2015) 094307.
- [36] F. Buendia, M.R. Beltran, X. Zhang, G. Liu, A. Buytendyk, K.H. Bowen, *Phys. Chem. Chem. Phys.* 17 (2015) 28219.
- [37] X. Zhang, G. Liu, G. Gantefoer, K.H. Bowen, A.N. Alexandrova, *J. Phys. Chem. Lett.* 5 (2014) 1596.
- [38] X. Zhang, G. Gantefoer, K.H. Bowen, A. Alexandrova, *J. Chem. Phys.* 140 (2014) 164316.
- [39] H. Wang, Y. Ko, X. Zhang, G. Gantefoer, H. Schnoekel, B.W. Eichhorn, P. Jena, B. Kiran, A.K. Kandalam, K.H. Bowen, *J. Chem. Phys.* 140 (2014) 124309.
- [40] H. Wang, X. Zhang, J. Ko, A. Grubisic, X. Li, G. Ganteför, H. Schnöckel, B. Eichhorn, M. Lee, P. Jena, A. Kandalam, B. Kiran, K.H. Bowen, *J. Chem. Phys.* 140 (2014) 054301.
- [41] A. Buytendyk, J. Graham, H. Wang, X. Zhang, E. Collins, Y.J. Ko, G. Gantefoer, B. Eichhorn, A. Regmi, K. Boggavarapu, K.H. Bowen, *Int. J. Mass Spectrom.* 365–366 (2014) 140.
- [42] X. Zhang, B. Visser, M. Tschurl, E. Collins, Y. Wang, Q. Wang, Y. Li, Q. Sun, P. Jena, G. Gantefoer, U. Boesl, U. Heiz, K.H. Bowen, *J. Chem. Phys.* 139 (2013) 111101.
- [43] J. Joseph, K. Pradhan, P. Jena, H. Wang, X. Zhang, Y.J. Ko, K.H. Bowen, *J. Chem. Phys.* 136 (2012) 194305.
- [44] A.S. Ivanov, X. Zhang, H. Wang, A.I. Boldyrev, G. Gantefoer, K.H. Bowen, I. Černušák, *J. Phys. Chem. A* 119 (2015) 11293.
- [45] A.D. Becke, *Phys. Rev. A* 38 (1988) 3098.
- [46] A.D. Becke, *J. Chem. Phys.* 98 (1993) 5648.
- [47] C. Lee, W. Yang, R.G. Parr, *Phys. Rev. B* 37 (1988) 785.
- [48] M.J. Risch, G.W. Trucks, H.B. Schlegel, G.E. Scuseria, M.A. Robb, J.R. Cheeseman, G. Scalmani, V. Barone, B. Mennucci, G.A. Petersson, et al., Gaussian 09, Revision A, Gaussian Inc., Wallingford, CT, 2009.
- [49] H. Wu, X. Li, X. Wang, C. Ding, L. Wang, *J. Chem. Phys.* 109 (1998) 449.
- [50] S.R. Desai, H. Wu, C.M. Rohlfing, L. Wang, *J. Chem. Phys.* 106 (1997) 1309.